



UNIVERSITY OF LEEDS

This is a repository copy of *A Schottky Barrier Device on Steel for use in Photovoltaics*.

White Rose Research Online URL for this paper:
<http://eprints.whiterose.ac.uk/99505/>

Version: Accepted Version

Proceedings Paper:

Ryall, N, Crook, R and Weinstein, JA (2016) A Schottky Barrier Device on Steel for use in Photovoltaics. In: PVSAT-12. PVSAT-12: Photovoltaic Science, Application and Technology Conference, 06-08 Apr 2016, Liverpool, UK. .

Reuse

Unless indicated otherwise, fulltext items are protected by copyright with all rights reserved. The copyright exception in section 29 of the Copyright, Designs and Patents Act 1988 allows the making of a single copy solely for the purpose of non-commercial research or private study within the limits of fair dealing. The publisher or other rights-holder may allow further reproduction and re-use of this version - refer to the White Rose Research Online record for this item. Where records identify the publisher as the copyright holder, users can verify any specific terms of use on the publisher's website.

Takedown

If you consider content in White Rose Research Online to be in breach of UK law, please notify us by emailing eprints@whiterose.ac.uk including the URL of the record and the reason for the withdrawal request.



eprints@whiterose.ac.uk
<https://eprints.whiterose.ac.uk/>

A Schottky Barrier Device on Steel for use in Photovoltaics

Niamh Ryall^{a*}, Rolf Crook^a and Julia Weinstein^b

^a Centre for Integrated Energy Research, University of Leeds, ^b Department of Chemistry, University of Sheffield

*Corresponding author: elner@leeds.ac.uk

Introduction

On bringing a metal and a semiconductor into contact, a diodic interface can be created, the Schottky barrier. Photovoltaic devices based on the sensitization of a Schottky barrier have been reported. [1] In these devices, the proposed mechanism is electron harvesting of electrons injected over a Schottky barrier interface into a semi-conductor film (Figure 1). This mechanism exploits the relatively long mean free path of hot electrons through a noble metal film.

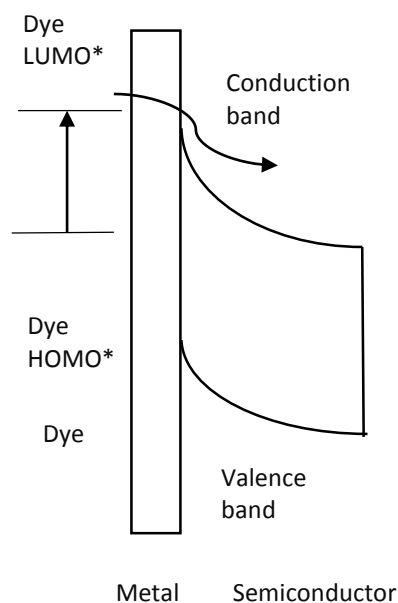


Figure 1: Principles of a Schottky barrier cell operating by thermionic emission through a thin metal barrier.

Similarly, a working photovoltaic cell was constructed using a "sandwich" of colloidal PbSe nanocrystals between a conductive transparent electrode and an evaporated metal contact. [2] However, this cell was not stable in air, showing a loss of its diodic characteristics within a few minutes.

Further, Schottky barriers formed between TiO₂ and noble metals have been studied in depth, and provide special interest as they offer the potential to functionalise the TiO₂ with dyes synthesised for Dye Sensitized Solar Cells. A device was fabricated from compact TiO₂ on a conductive transparent substrate with a 100 nm sputtered gold top contact. These devices were functionalised with Ru(dcbpy)₂(NCS)₂ dye (where dcbpy is (2,2'-bipyridine)-4,4'-dicarboxylic acid). These cells showed improved rectification and an improved photocurrent compared to the unfunctionalised cells. [3] The authors consider the formation of oxygen vacancies to be important in the formation of the barrier and the impact of the dye binding is likely to be due to the effect the dye has on the oxygen vacancies. [3] The Schottky barrier has also been employed directly in Dye Sensitized Solar Cells by the deposition of gold nanoparticles on ZnO anodes, the Schottky barrier is thought to reduce the recombination of electrons with the oxidised dye or electrolyte, improving the efficiency.[4]

Previous work in this group has shown it is possible to achieve a small visible photoresponse from a Schottky barrier device synthesised from a thermally grown TiO₂ layer on electropolished titanium followed by deposition of silver nanowires and functionalisation with nanocrystals. [5]

In this work we report the fabrication and initial characterisation of Schottky-barrier solar cells built up from a 304 stainless steel substrate. The Schottky barrier forms at the interface between a TiO₂ nanoparticle layer and an Ag nanowire mesh. TiO₂ sols were used to form a TiO₂ layer on stainless steel. On this, silver nanowires were deposited. The Schottky barrier formed between TiO₂ and the silver nanomesh was characterised with current-voltage (IV) measurements. The devices were modified with a dye and small molecules, showing some limited photocurrent and improved reverse

saturation currents. After modification of the film and passivation together, high photocurrents were seen (up to 10% EQE at 300 nm).

Experimental

In a typical sol synthesis, 12 ml of IPA, 1 ml of distilled water and 1 ml nitric acid are stirred vigorously. 0.5 ml of titanium isopropoxide is then added dropwise. This is stirred for at least 30 minutes, yielding a pale yellow transparent viscous liquid. Following this, ammonia solution (30%) is added dropwise with stirring until pH paper shows the sol is neutral. Typically, the sol is cloudy and viscous above pH 4 or 5 as this is above the isoelectric point of the TiO₂ particles. The steel is chopped into small (~1cm²) pieces and washed with IPA to remove any surface grease. It is then dipped into the sol and removed. The excess sol drains away via capillary action when the device is placed on its side on a piece of lab tissue. This first layer is left to dry at room temperature and the dipping process is repeated once more. For an anatase layer, the sol is hydrolysed for 8 hours under reflux before neutralisation. The TiO₂ films are then sintered at 350 °C for 90 minutes in a furnace. When cool, the device are drop cast with a commercial 0.25% silver nanowire (60 nm diameter × 10 μm length) suspension in isopropanol, via a micropipette, in intervals of 5 μL. Typically 10-25 μL of AgNWs are used per device, to guarantee a good contact. The silver nanowires are annealed at 235 °C for 20 minutes to reduce junction resistance. The current-voltage measurements have been performed on a Gamry Potentiostat between -1 V and 1V, using a 100 Ohm resistor in series to limit the current travelling through the device. Photocurrents have been measured using an arc lamp (Bentham SSM150Xe Programmable light source) controlled with a program written in-house by R.Crook, calibrated with a commercial Si photodiode (ThorLabs FDS100 Si Photodiode). Mathematical analysis of the IV measurements was performed with MatLab. All reagents were purchased from Sigma Aldrich and used without further purification.

Results and discussion

The cells synthesised in this way show an incomplete TiO₂ layer, though this does not adversely affect the cells (Figures 2 and 3). The high aspect ratio of the silver nanowires results in them lying on the surface, not touching the back contact.

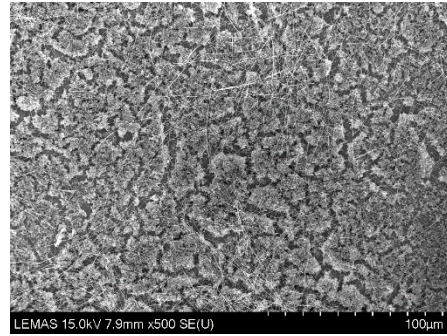


Figure 2: TiO₂ film on steel, showing a plate-like structure with gaps.

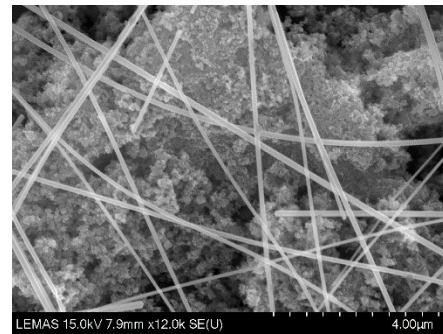


Figure 3: Silver nanowire mesh on porous TiO₂ structure.

Recent results, showing the devices showing Ohmic behaviour at low temperatures, before showing diodic properties above ~150 °C, see Figures (4, 5).

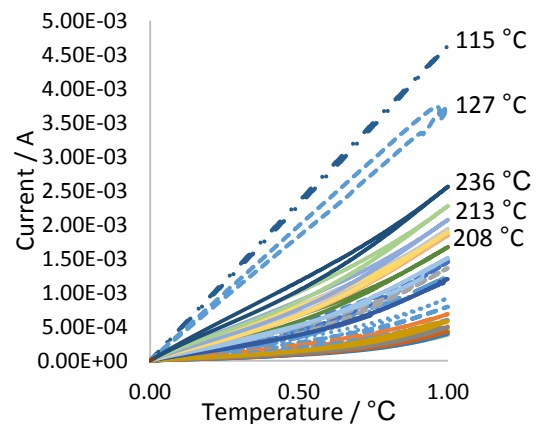


Figure 4: Forward bias IV curves for increasing temperatures. Dashed lines were recorded up to 200 °C, solid lines up to 271 °C. Some indicative temperatures are shown.

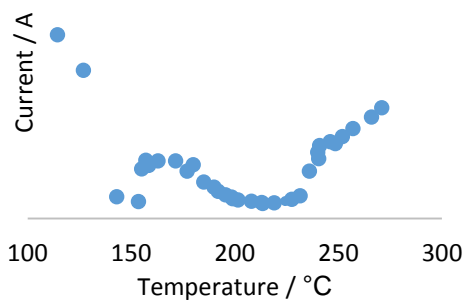


Figure 5: The current measured at 1.0 V for a device at increasing temperatures.

From this, it appears that the initial Ohmic behaviour gave way to formation of the Schottky barrier. This may be due to the removal of solvents used in deposition. There is a slow increase in current, possibly due to a reduction in the nanomesh resistance or an increase in leakage current mechanisms due to diffusion of metal from the steel or silver nanowires.

The devices were analysed using Matlab by a simple exponential fit to the ideal diode equation, equation (1).

$$J = J_0 \left(\left(\exp \frac{qV}{nkT} \right) - 1 \right) \quad (1)$$

Where J is the measured current, J_0 is the reverse saturation current, V is the applied voltage, n is the ideality factor and q/kT has its usual meaning.

From this simple model, reasonably high R^2 values were obtained, the results in Figure 6 were fits where the R^2 values were over 0.90 (light grey), 0.95 (dark grey) and 0.99 (black). These results represent a range of devices made whilst working on the fabrication method, for instance, the black markers represent 189 cells and 425 measurements.

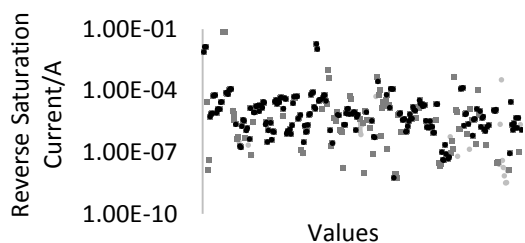


Figure 6: Reverse saturation currents for devices showing typical values between 1×10^{-4} to 10^{-8} .

The modification of the device to include $\text{Ru}(\text{dcbpy})_2(\text{NCS})_2$ dye resulted in better I_0 values, from an average for a control batch made previously, giving an average I_0 value for the batch

(6 devices, 17 measurements) of 3.60×10^{-7} . The range of this batch was lower than the control devices. It was also possible to measure a small photocurrent under visible light wavelengths (Figure 7) for these cells.

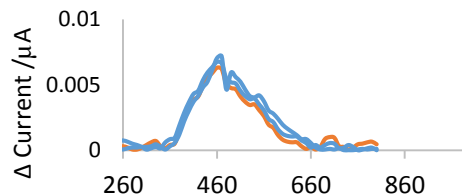


Figure 7: Small photocurrents measured for devices functionalised with $\text{Ru}(\text{dcbpy})_2(\text{NCS})_2$ dye. The majority of the absorption occurs in the visible region, where the TiO_2 does not absorb light.

The Schottky barrier extends in three dimensions, and so the injection of electrons into the conduction band may not involve ballistic transport (Figure 8).

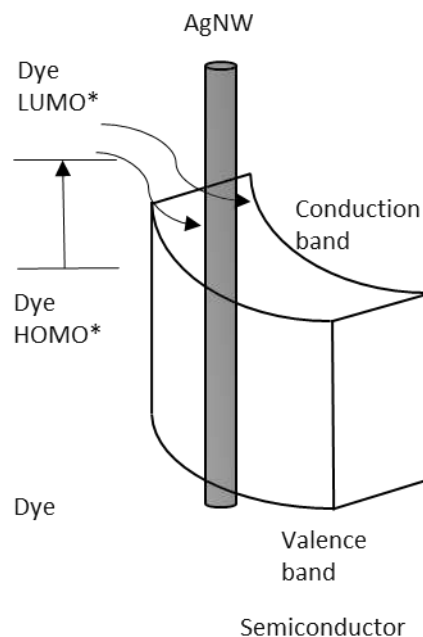


Figure 8: Diagram of Schottky barrier cell demonstrating the potential electron transfer mechanisms to the conduction band of a semiconductor.

The photoresponse is seen at longer wavelengths than the absorption band of TiO_2 demonstrating the importance of the dye to visible light absorption. That the unfunctionalised device does not show a UV response, suggests that the success of the dye sensitized device when compared to the

unfunctionalised device is likely also due to the effect of the passivation of surface states on the TiO₂, as noted by previous authors. [3] These work was using an amorphous TiO₂ layer and recent work has shown that cells fabricated from an anatase sol, then passivated with tartaric acid gave better photoresponses (Figure 8), with good external quantum efficiencies (Figure 9) in the UV region, demonstrating the importance of fabrication method and passivation in these cells.

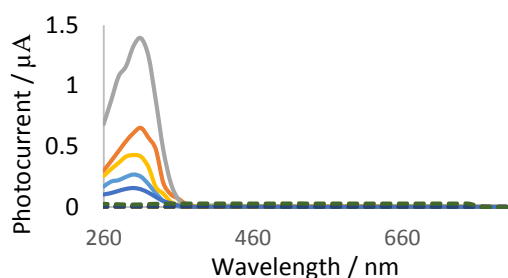


Figure 9: Photocurrents measured in the UV for tartaric acid functionalised devices for a range of devices, before (dashed lines) and after (solid lines) functionalisation.

For comparison, the commercial silicon photodiode had a maximum output of 31 μA at ~500 nm, however, as can be seen in Figure 10, the output of the lamp decreases with shorter wavelengths.

The EQE is high when compared to the typical geometric coverage of silver nanowires of ~13% by area for these devices.

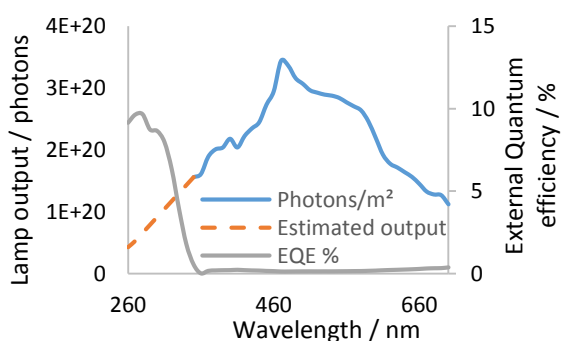


Figure 10: Calibrated output for the arc lamp is shown in blue (solid line). Orange (dashes) is the estimated output between 350 and 260 nm, and the external quantum efficiency, calculated from the estimated output.

Conclusion

In this work, a large area Schottky barrier device was synthesised under standard laboratory

conditions with no specialist equipment from TiO₂ and commercial silver nanowires. These devices are stable for at least many months. The photocurrents from the unmodified devices are very low, though the Ru(dcbpy)₂(NCS)₂ dye shows some improved results. The best photocurrents were seen for passivated devices fabricated with a sol which had been hydrolysed. The improved devices could provide a good device to be functionalised with nanocrystals, as has been done previously in this group, or dyes.

Estimations of efficiency are likely to be too low due to the likely faster drop in output at UV wavelengths and the unknown absorption of UV light by optical fibres used in the experiment.

Further work is required on the diffusion and passivation phenomena which are important in these devices.

The ability to separate charges across this interface could also be of interest in catalysis or sensing applications as devices such as these have been used in gas and photo sensing applications.

References

- [1] E.W. McFarland and J. Tang, Nature, 2003, **421**, 616-618
- [2] J.M. Luther et al., Nano Letters, 2008, **8**, 3488-3492
- [3] Th. Dittrich et al., Thin Solid Films, 2008, **516**, 7234-7236
- [4] T. Bora et al., 2011, Beilstein Journal of Nanotechnology, **2**, 681-690
- [5] D. Jaques, Demonstration and Evaluation of a Nanocrystal-Nanowire Solar Cell, 2015, PhD Thesis, University of Leeds